arXiv:0903.3823v1 [hep-ph] 23 Mar 2009

Scalar, axial-vector and tensor resonances from the ρD^*, ωD^* interaction in the hidden gauge formalism.

R. Molina[1], H. Nagahiro[2,3], A. Hosaka[3] and E. Oset[1]

March 23, 2009

[1] Departamento de Física Teórica and IFIC, Centro Mixto Universidad de Valencia-CSIC,
Institutos de Investigación de Paterna, Aptdo. 22085, 46071 Valencia, Spain
[2] Department of Physics, Nara Women's University, Nara 630-8506, Japan
[3] Research Center for Nuclear Physics (RCNP), Osaka University, Ibaraki, Osaka
567-0047, Japan

Abstract

We study composite systems of light (ρ and ω) and heavy (D^*) vector mesons by using the interaction within the hidden gauge formalism. We find a strong attraction in the isospin, spin channels $(I, S) = (1/2, 0)$; $(1/2, 1)$; $(1/2, 2)$ with positive parity. The attraction is large enough to strongly bind these mesons in states with these quantum numbers, leading to states which can be identified with $D_2^*(2460)$ and probably with $D^*(2640)$, the last one without experimental spin and parity assignment. In the case of $I = 3/2$ one obtains repulsion and thus, no exotic mesons in this sector are generated in the approach.

1 Introduction

Recently a study of the $\rho\rho$ interaction with the hidden gauge formalism [1, 2, 3] was carried out in [3]. The hidden gauge symmetry (HGS) was introduced by Bando-Kugo-Yamawaki where the ρ meson was regarded as a dynamical gauge boson of the HGS of the nonlinear sigma model. One of interesting facts which is relevant in the present discussion is that there is a strong attraction in the isospin and spin channels $(I, S) = (0, 0)$ and $(0, 2)$, which is enough to bind the $\rho\rho$ system leading to a tensor and a scalar meson which could be identified with the $f_0(1370)$ and $f_2(1270)$ meson states [4]. In a later work the radiative decay of these states in $\gamma\gamma$, a channel with rates very sensitive to the nature of the resonances, was studied [5] obtaining results in agreement with the PDG [6] for the case of the tensor state and in qualitative agreement with preliminary results at Belle for the scalar state [7]. The work of [3] has been recently extended to SU(3) for the interaction of the vectors of the nonet, where several states, which can be identified with existing resonances are also dynamically generated [8]. The success of the approach encourages us to study the charm sector in the lightest case, the one for the interaction of the ρ, ω and D^* mesons. Another possible approach to this work could be done following the lines of [9] for meson-baryon interaction involving $SU(8)$ symmetry. Work in this direction is in progress [10] but we can advance that while for pseudoscalar-baryon interaction the approaches are equivalent, when vector meson are involved the results are very different [11].

The starting point in our approachis the interaction of vector mesons among themselves provided by the hidden gauge formalism, which now has to be generalized to SU(4) to accommodate the charm vectors D^* into the framework. Admitting that SU(4) is more strongly broken than SU(3), the SU(4) symmetry is invoked in the basic hidden gauge Lagrangians but is already broken in the vector exchange diagrams that provide the amplitudes for the vector-vector interaction. What we find is a strong attraction in the isospin, spin channels $(I, S) = (1/2, 0)$; $(1/2, 1)$; $(1/2, 2)$; which leads to bound $\rho(\omega)D^*$ states in all these channels. In the case of $I = 3/2$ we find repulsion and hence we do not generate states that would qualify as exotic from the $q\bar{q}$ picture. The states that we find qualify as mostly ρD^* molecules, and fit nicely with the experimental states $D_2^*(2460)$ and $D^*(2640)$. The present study would, thus, suggest for these states a different nature than the one usually assumed in terms of $q\bar{q}$ states [6, 12, 13].

2 Formalism for VV interaction

2.1 Lagrangian

We follow the formalism of the hidden gauge symmetry (HGS) for vector mesons of [1, 2](see also [14] for a practical set of Feynman rules). The Lagrangian involving the interaction of vector mesons amongst themselves is given by

$$\mathcal{L}_{III} = -\frac{1}{4}\langle V_{\mu\nu} V^{\mu\nu} \rangle \ , \tag{1}$$

where the symbol $\langle\rangle$ stands for the trace in the $SU(4)$ space and $V_{\mu\nu}$ is given by

$$V_{\mu\nu} = \partial_\mu V_\nu - \partial_\nu V_\mu - ig[V_\mu, V_\nu] \ , \tag{2}$$

with g given by

$$g = \frac{M_V}{2f} \ , \tag{3}$$

and $f = 93\, MeV$ the pion decay constant. The value of g of Eq. (3) is one of the ways to account for the KSFR relation [15] which is tied to vector meson dominance [16]. The vector field V_μ is represented by the $SU(4)$ matrix which is parameterized by 16 vector

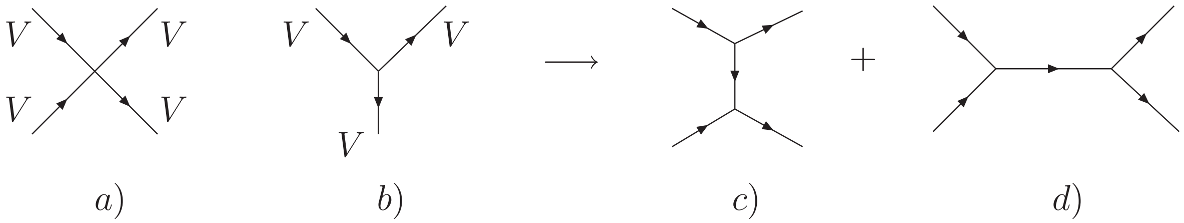

Figure 1: Terms of the $\mathcal{L}_{III}$ Lagrangian: a) four vector contact term, Eq. (5); b) three-vector interaction, Eq. (6); c) t and u channels from vector exchange; d) s channel for vector exchange.

mesons including 15-plet and singlet of $SU(4)$,

$$V_\mu = \left(\begin{array}{cccc} \frac{\rho^0}{\sqrt{2}} + \frac{\omega}{\sqrt{2}} & \rho^+ & K^{*+} & \bar{D}^{*0} \\ \rho^- & -\frac{\rho^0}{\sqrt{2}} + \frac{\omega}{\sqrt{2}} & K^{*0} & D^{*-} \\ K^{*-} & \bar{K}^{*0} & \phi & D_s^{*-} \\ D^{*0} & D^{*+} & D_s^{*+} & J/\psi \end{array} \right)_\mu , \tag{4}$$

where the ideal mixing has been taken for ω, ϕ and J/ψ. The interaction of $\mathcal{L}_{III}$ gives rise to a contact term coming for $[V_\mu, V_\nu][V_\mu, V_\nu]$

$$\mathcal{L}_{III}^{(c)} = \frac{g^2}{2} \langle V_\mu V_\nu V^\mu V^\nu - V_\nu V_\mu V^\mu V^\nu \rangle , \tag{5}$$

depicted in Fig. 1 a), and on the other hand it gives rise to a three vector vertex

$$\mathcal{L}_{III}^{(3V)} = ig \langle (\partial_\mu V_\nu - \partial_\nu V_\mu) V^\mu V^\nu \rangle , \tag{6}$$

depicted in Fig. 1 b). This latter Lagrangian gives rise to a $VV \to VV$ interaction by means of the exchange of one of the vectors, as shown in Fig. 1 c).

The $SU(4)$ structure of the Lagrangian allows us to take into account all the channels within $SU(4)$ which couple to certain quantum numbers. In the present work we shall present results for the case of the ρD^* interaction. The formalism is the same used in [4]. Some approximations were made there which make the formalism handy and reliable, by neglecting the three-momentum of the vector mesons with respect to their masses. It is interesting to see that with this approximation one obtains [14] from the hidden gauge approach the chiral local Lagrangians which are used to study the interaction of pseudoscalar mesons among themselves and the pesudoscalar mesons with vector mesons and with baryons [17, 18].

2.2 Four-vector contact interaction

Starting with the Lagrangian of Eq. (5) we can immediately obtain the amplitude of, for instance, $\rho^+ D^{*0} \to \rho^+ D^{*0}$ corresponding to Fig. 2, in the particle base,

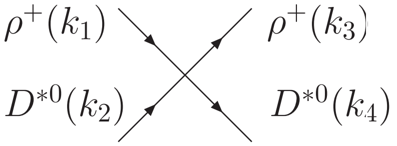

Figure 2: Contact term of the $\rho\rho$ interaction.

$$-it^{(c)}_{\rho^+D^{*0}\to\rho^+D^{*0}} = ig^2(2\epsilon^{(1)}_\mu\epsilon^{(2)}_\nu\epsilon^{(3)\,\nu}\epsilon^{(4)\,\mu} - \epsilon^{(1)}_\mu\epsilon^{(2)}_\mu\epsilon^{(3)\,\nu}\epsilon^{(4)\,\nu} - \epsilon^{(1)}_\nu\epsilon^{(2)}_\mu\epsilon^{(3)\,\nu}\epsilon^{(4)\,\mu}) \;, \tag{7}$$

where the indices $1, 2, 3$ and 4 correspond to the particles with momenta k_1, k_2, k_3 and k_4 in Fig. 2. It is straightforward to write down all amplitudes for other channels.

In the approximation of neglecting the three-momenta of the vector mesons, only the spatial components of the polarization vectors are nonvanishing and then one can obtain easily spin projection operators [4] into spin 0, 1, 2 states, which are given below:

$$\begin{aligned}\mathcal{P}^{(0)} &= \frac{1}{3}\epsilon_\mu\epsilon^\mu\epsilon_\nu\epsilon^\nu \\ \mathcal{P}^{(1)} &= \frac{1}{2}(\epsilon_\mu\epsilon_\nu\epsilon^\mu\epsilon^\nu - \epsilon_\mu\epsilon_\nu\epsilon^\nu\epsilon^\mu) \\ \mathcal{P}^{(2)} &= \{\frac{1}{2}(\epsilon_\mu\epsilon_\nu\epsilon^\mu\epsilon^\nu + \epsilon_\mu\epsilon_\nu\epsilon^\nu\epsilon^\mu) - \frac{1}{3}\epsilon_\mu\epsilon^\mu\epsilon_\nu\epsilon^\nu\} \;,\end{aligned} \tag{8}$$

where the order 1, 2, 3, 4 in the polarization vectors is understood. We can then write the combination of polarization vectors appearing in Eq. (7) in terms of the spin combinations and thus we obtain the kernel of the interaction which will be later on used to solve the Bethe-Salpeter equation. However, it is practical to construct the isospin combinations before the spin projection is done.

Recalling that we have an isospin doublet with $(-D^{*0}, D^{*+})$ and one isospin triplet, $(\rho^-, \rho^0, -\rho^+)$, the $I = 1/2$ and $3/2$ combinations are written as

$$\begin{aligned}|\rho D^*, I = 1/2, I_3 = 1/2\rangle &= \sqrt{\frac{2}{3}}|\rho^+D^{*0}\rangle - \frac{1}{\sqrt{3}}|\rho^0D^{*+}\rangle, \\ |\rho D^*, I = 1/2, I_3 = 3/2\rangle &= \frac{1}{\sqrt{3}}|\rho^+D^{*0}\rangle + \sqrt{\frac{2}{3}}|\rho^0D^{*+}\rangle \;.\end{aligned} \tag{9}$$

We then find the amplitudes in the isospin base by forming linear combinations of the amplitudes in the particle base weighted by the Clebsh-Gordan coefficients as given in Eq. (9),

$$\begin{aligned}t^{(I=1/2)} &= g^2(-\frac{7}{2}\epsilon_\mu\epsilon_\nu\epsilon^\nu\epsilon^\mu + \frac{5}{2}\epsilon_\mu\epsilon^\mu\epsilon_\nu\epsilon^\nu + \epsilon_\mu\epsilon_\nu\epsilon^\mu\epsilon^\nu) \;, \\ t^{(I=3/2)} &= g^2(\epsilon_\mu\epsilon_\nu\epsilon^\nu\epsilon^\mu + \epsilon_\mu\epsilon_\nu\epsilon^\mu\epsilon^\nu - 2\epsilon_\mu\epsilon^\mu\epsilon_\nu\epsilon^\nu) \;.\end{aligned} \tag{10}$$

These amplitudes, after projection into the spin channels, give rise to the following kernels (potential) for $I = 1/2$,

$$\begin{aligned} t^{(I=1/2,S=0)} &= +5g^2 \ , \\ t^{(I=1/2,S=1)} &= +\frac{9}{2}g^2 \ , \\ t^{(I=1/2,S=2)} &= -\frac{5}{2}g^2 \ , \end{aligned} \tag{11}$$

and also for the case of $I = 3/2$,

$$\begin{aligned} t^{(I=3/2,S=0)} &= -4g^2 \ , \\ t^{(I=3/2,S=1)} &= 0 \ , \\ t^{(I=3/2,S=2)} &= +2g^2 \ . \end{aligned} \tag{12}$$

When one or two ρ meson(s) are replaced by the ω meson(s), where is only one isospin state $I = 1/2$, we find the following interaction terms,

$$\begin{aligned} t^{(I=1/2)}_{\rho D^* \to \omega D^*} &= \frac{\sqrt{3}}{2}g^2(2\epsilon_\mu\epsilon_\nu\epsilon^\mu\epsilon^\nu - \epsilon_\mu\epsilon_\nu\epsilon^\nu\epsilon^\mu - \epsilon_\mu\epsilon^\mu\epsilon_\nu\epsilon^\nu) \ , \\ t^{(I=1/2)}_{\omega D^* \to \omega D^*} &= -\frac{1}{2}g^2(\epsilon_\mu\epsilon_\nu\epsilon^\nu\epsilon^\mu + \epsilon_\mu\epsilon^\mu\epsilon_\nu\epsilon^\nu - 2\epsilon_\mu\epsilon_\nu\epsilon^\mu\epsilon^\nu) \ . \end{aligned} \tag{13}$$

After projection in spin they become for $\rho D^* \to \omega D^*$,

$$\begin{aligned} t^{(I=1/2,S=0)}_{\rho D^* \to \omega D^*} &= -\sqrt{3}g^2 \ , \\ t^{(I=1/2,S=1)}_{\rho D^* \to \omega D^*} &= +\frac{3\sqrt{3}}{2}g^2 \ , \\ t^{(I=1/2,S=2)}_{\rho D^* \to \omega D^*} &= +\frac{\sqrt{3}}{2}g^2 \ , \end{aligned} \tag{14}$$

and in the same way, we have for $\omega D^* \to \omega D^*$,

$$\begin{aligned} t^{(I=1/2,S=0)}_{\omega D^* \to \omega D^*} &= -g^2 \ , \\ t^{(I=1/2,S=1)}_{\omega D^* \to \omega D^*} &= +\frac{3}{2}g^2 \ , \\ t^{(I=1/2,S=2)}_{\omega D^* \to \omega D^*} &= +\frac{1}{2}g^2 \ . \end{aligned} \tag{15}$$

2.3 ρ meson exchange terms

From the Lagrangian of Eq. (6) we get the three-vector vertex as depicted in Fig. 3. For practical purposes it is convenient to rewrite the three-vector Lagrangian of Eq. (6) as,

$$\begin{aligned} \mathcal{L}^{(3V)}_{III} &= ig\langle V^\nu\partial_\mu V_\nu V^\mu - \partial_\nu V_\mu V^\mu V^\nu\rangle \\ &= ig\langle (V^\mu\partial_\nu V_\mu - \partial_\nu V_\mu V^\mu)V^\nu\rangle \ . \end{aligned} \tag{16}$$

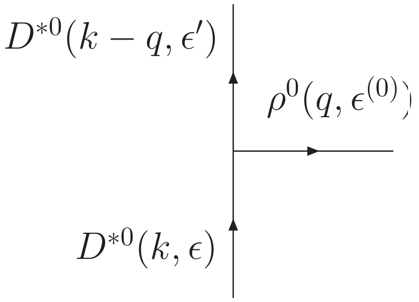

Figure 3: three-vector vertex diagram.

In Eq. (16) we have a three-vector vertex, where any of the three vector fields can correspond in principle to the exchanged vector in the diagram of Fig. 1(c). Nevertheless, by assuming that the three-momenta of the external vectors can be neglected as compared with the vector mass, the polarization vectors of the external vector mesons have only spatial components. Then by looking at the Lagrangian of Eq. (16) we see that the field V^ν cannot correspond to an external vector meson. Indeed, if this were the case, the ν index must be spatial and then the partial derivative ∂_ν is replaced by a three-momentum of the vector mesons which is neglected in the approach. Then V^ν corresponds to the exchanged vector and this simplifies the calculation. The approximation of neglecting the three-momenta of the external vectors corresponds to the consideration of only the s-wave.

The vertex function corresponding to the diagram of Fig. 3 is given by

$$\begin{aligned} -it^{(3)} = &- \frac{g}{\sqrt{2}}\{(iq_\mu\epsilon^{(0)}_\nu - iq_\nu\epsilon^{(0)}_\mu)\epsilon'^\mu\epsilon^\nu \\ &+ (i(k-q)_\mu\epsilon'_\nu - i(k-q)_\nu\epsilon'_\mu)\epsilon^\mu\epsilon^{(0)\nu} \\ &+ (-ik_\mu\epsilon_\nu + ik_\nu\epsilon_\mu)\epsilon^{(0)\mu}\epsilon'^\nu\}\ . \end{aligned} \tag{17}$$

With this basic structure we can readily evaluate the amplitude of the first diagram of Fig. 4 to obtain

$$\begin{aligned} -it^{(ex)}_{\rho^+D^{*0}\to\rho^+D^{*0}} = &- \sqrt{2}g\{(-i(k_3-k_1)_\mu\epsilon^{(0)}_\nu + i(k_3-k_1)_\nu\epsilon^{(0)}_\mu)\epsilon^{(1)\mu}\epsilon^{(3)\nu} \\ &+ (-ik_{1\mu}\epsilon^{(1)}_\nu + ik_{1\nu}\epsilon^{(1)}_\mu)\epsilon^{(3)\mu}\epsilon^{(0)\nu} + (ik_{3\mu}\epsilon^{(3)}_\nu - ik_{3\nu}\epsilon^{(3)}_\mu)\epsilon^{(0)\mu}\epsilon^{(1)\nu}\} \\ &\times \frac{i}{(k_3-k_1)^2 - M_\rho^2 + i\epsilon} \\ &\times -\frac{g}{\sqrt{2}}\{(i(k_2-k_4)_\mu\epsilon^{(0)}_\nu - i(k_2-k_4)_\nu\epsilon^{(0)}_\mu)\epsilon^{(4)\mu}\epsilon^{(2)\nu} \\ &+ (ik_{4\mu}\epsilon^{(4)}_\nu - ik_{4\nu}\epsilon^{(4)}_\mu)\epsilon^{(2)\mu}\epsilon^{(0)\nu} \\ &+ (-ik_{2\mu}\epsilon^{(2)}_\nu + ik_{2\nu}\epsilon^{(2)}_\mu)\epsilon^{(0)\mu}\epsilon^{(4)\nu}\}\ . \end{aligned} \tag{18}$$

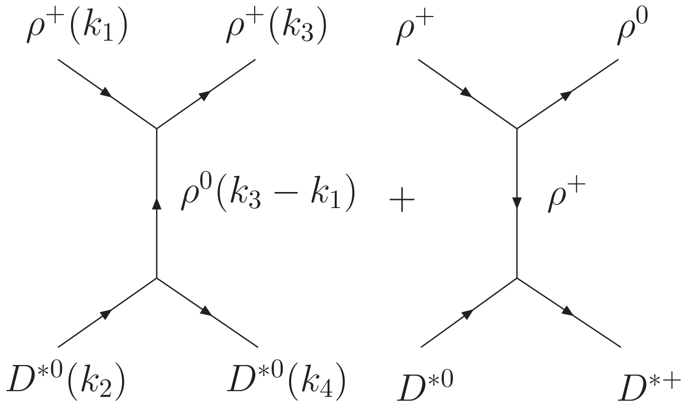

Figure 4: Vector exchange diagrams for $\rho D^* \to \rho D^*$.

Recalling that the three-momenta of the external particles is small and neglected, we arrive at the following expression:

$$t^{(ex)}_{\rho^+ D^{*0}\to\rho^+ D^{*0}} = -\frac{g^2}{M_\rho^2}\,(k_1+k_3)\cdot(k_2+k_4)\,\epsilon_\mu\epsilon_\nu\epsilon^\mu\epsilon^\nu \ . \tag{19}$$

By looking at the structure of the second diagram in Fig. 4 we find the following result for the amplitude:

$$t^{(ex)}_{\rho^+ D^{*0}\to\rho^0 D^{*+}} = \sqrt{2}\,\frac{g^2}{M_\rho^2}\,(k_1+k_3)\cdot(k_2+k_4)\,\epsilon_\mu\epsilon_\nu\epsilon^\mu\epsilon^\nu. \tag{20}$$

We note that the amplitude $\rho^0 D^* \to \rho^0 D^*$ with ρ^0 exchange vanishes because the three-ρ^0 vertex does not exist due to isospin invariance. We can see that in all the cases the combination of vector polarizations is the same. The isospin projections give us

$$\begin{aligned} t^{(ex,I=1/2)}_{\rho D^*\to\rho D^*} &= -2\,\frac{g^2}{M_\rho^2}\,(k_1+k_3)\cdot(k_2+k_4)\,\epsilon_\mu\epsilon_\nu\epsilon^\mu\epsilon^\nu \ , \\ t^{(ex,I=3/2)}_{\rho D^*\to\rho D^*} &= \frac{g^2}{M_\rho^2}\,(k_1+k_3)\cdot(k_2+k_4)\,\epsilon_\mu\epsilon_\nu\epsilon^\mu\epsilon^\nu \ . \end{aligned} \tag{21}$$

Now using the equations for the spin projections we can split the terms into their spin parts and we obtain

$$\begin{aligned} t^{(ex,I=1/2,S=0,1,2)}_{\rho D^*\to\rho D^*} &= -2\,\frac{g^2}{M_\rho^2}\,(k_1+k_3)\cdot(k_2+k_4) \ , \\ t^{(ex,I=3/2,S=0,1,2)}_{\rho D^*\to\rho D^*} &= \frac{g^2}{M_\rho^2}\,(k_1+k_3)\cdot(k_2+k_4) \ , \end{aligned} \tag{22}$$

that is: we find spin degeneration in the amplitudes which involve the exchange of one ρ meson. These structures can be simplified using momentum conservation and one finds:

$$\begin{aligned} t^{(ex,I=1/2,S=0,1,2)}_{\rho D^*\to\rho D^*} &= - \; 2\,\frac{g^2}{M_\rho^2}\,\{\frac{3}{2}s - m_\rho^2 - m_{D^*}^2 - \frac{(m_\rho^2 - m_{D^*}^2)^2}{2s}\}\ , \\ t^{(ex,I=3/2,S=0,1,2)}_{\rho D^*\to\rho D^*} &= + \; \frac{g^2}{M_\rho^2}\,\{\frac{3}{2}s - m_\rho^2 - m_{D^*}^2 - \frac{(m_\rho^2 - m_{D^*}^2)^2}{2s}\}\ . \end{aligned} \tag{23}$$

Note that for the exchange of a vector we do not have contribution from the ωD^* channel. Indeed, the vertex $\omega\omega\omega$ and $\rho\rho\omega$ violate G-parity, and the the $\rho\omega\omega$ violates isospin. In the next section we consider the amplitudes which include also the exchange of one heavy vector meson, but we anticipate that the amplitudes calculated so far are more relevant than the other ones.

2.4 D^*-exchange terms

In this section we are going to take into account the exchange of one heavy vector meson, D^* or $\bar{D}^*$, in the channels ρD^* and ωD^*, by means of the diagrams that we draw in Fig. 5. Note that in Fig. 5 the vertex $\omega\omega D^*$ does not appear because it violates isospin. By means of the Lagrangian of Eq. (6) we arrive at the following amplitudes for the first and second diagrams depicted in that figure,

$$\begin{aligned} t^{(D^*-ex)}_{\rho^+D^{*0}\to\rho^0D^{*+}} &= \frac{1}{\sqrt{2}}\frac{g^2}{M_{D^*}^2}\,(k_1+k_4)\cdot(k_2+k_3)\,\epsilon_\mu\epsilon_\nu\epsilon^\nu\epsilon^\mu \\ t^{(D^*-ex)}_{\rho^0D^{*+}\to\rho^0D^{*+}} &= \frac{1}{2}\frac{g^2}{M_{D^*}^2}\,(k_1+k_4)\cdot(k_2+k_3)\,\epsilon_\mu\epsilon_\nu\epsilon^\nu\epsilon^\mu\ . \end{aligned} \tag{24}$$

The isospin decomposition can be done as before by making weighted sums of Eq. (24). We find,

$$\begin{aligned} t^{(D^*-ex,I=1/2)}_{\rho D^*\to\rho D^*} &= -\frac{1}{2}\frac{\kappa\,g^2}{M_\rho^2}\,(k_1+k_4)\cdot(k_2+k_3)\,\epsilon_\mu\epsilon_\nu\epsilon^\nu\epsilon^\mu \\ t^{(D^*-ex,I=3/2)}_{\rho D^*\to\rho D^*} &= \frac{\kappa\,g^2}{M_\rho^2}\,(k_1+k_4)\cdot(k_2+k_3)\,\epsilon_\mu\epsilon_\nu\epsilon^\nu\epsilon^\mu. \end{aligned} \tag{25}$$

where $\kappa = M_\rho^2/M_{D^*}^2$. Upon spin projection we find,

$$\begin{aligned} t^{(D^*-ex,I=1/2,S=0,2)}_{\rho D^*\to\rho D^*} &= -\frac{1}{2}\frac{\kappa\,g^2}{M_\rho^2}\,(k_1+k_4)\cdot(k_2+k_3) \\ t^{(D^*-ex,I=1/2,S=1)}_{\rho D^*\to\rho D^*} &= \frac{1}{2}\frac{\kappa\,g^2}{M_\rho^2}\,(k_1+k_4)\cdot(k_2+k_3)\ , \end{aligned} \tag{26}$$

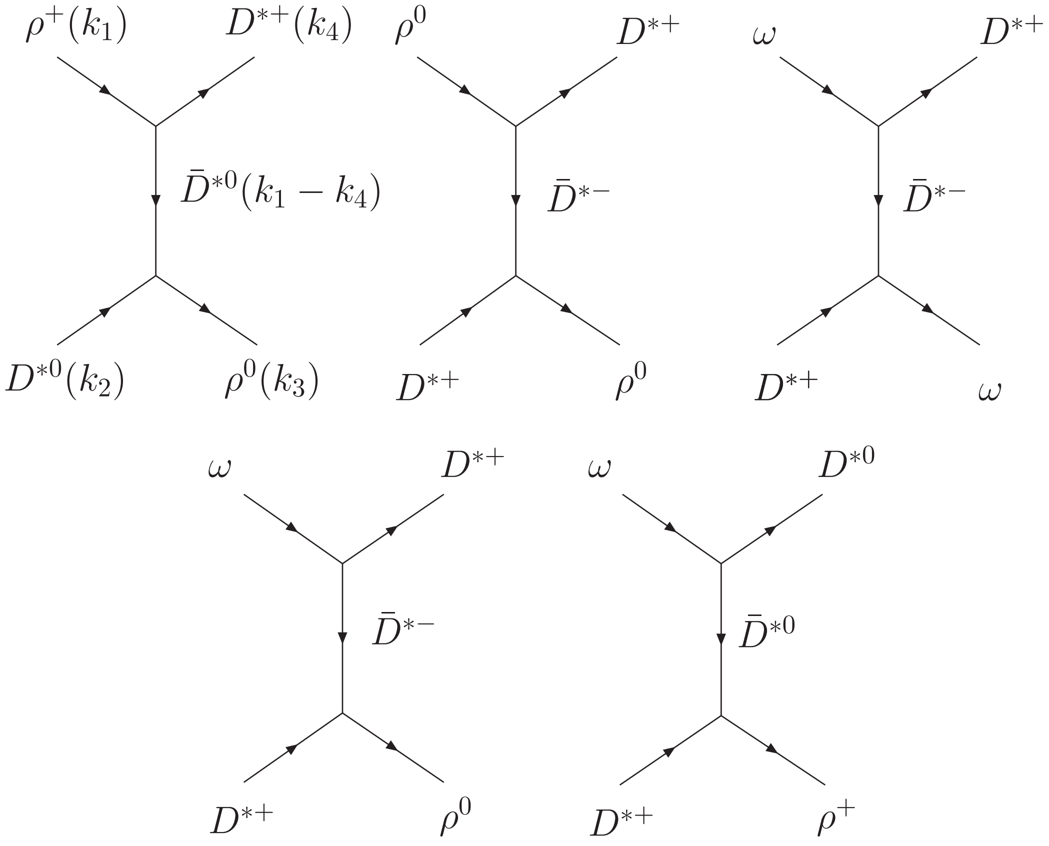

Figure 5: Diagrams including the exchange of one heavy vector meson.

and similarly for $I = 3/2$,

$$\begin{aligned} t^{(D^*-ex,I=3/2,S=0,2)}_{\rho D^*\to\rho D^*} &= \frac{\kappa\, g^2}{M_\rho^2}\,(k_1+k_4)\cdot(k_2+k_3) \\ t^{(D^*-ex,I=3/2,S=1)}_{\rho D^*\to\rho D^*} &= -\frac{\kappa\, g^2}{M_\rho^2}\,(k_1+k_4)\cdot(k_2+k_3)\ . \end{aligned} \tag{27}$$

Again by neglecting the three-momenta of the external particles and by taking the center-of-mass reference system, one can express the factors which involve momenta as

$$\begin{aligned} (k_1+k_3)\cdot(k_2+k_4) &= \frac{3}{2}s - m_\rho^2 - m_{D^*}^2 - \frac{(m_\rho^2-m_{D^*}^2)^2}{2s}\ , \\ (k_1+k_4)\cdot(k_2+k_3) &= \frac{3}{2}s - m_\rho^2 - m_{D^*}^2 + \frac{(m_\rho^2-m_{D^*}^2)^2}{2s}\ . \end{aligned} \tag{28}$$

As we can observe, the spin degeneracy seen in the ρ-meson exchange amplitudes is lost in the D^*-exchange amplitudes. However, it is broken only a little due to the suppressing factor $\kappa = m_\rho^2/m_{D^*}^2 \sim 0.15$.

The results are summarized in the columns titled "D^*-exchange" in Tables 1, 2 and 3. These new terms represent corrections of the order of 10% of the ρ-exchange ones. As can be observed in the total amplitudes, we find attraction in the sector $I = 1/2$, whereas the sector $I = 3/2$ turns out repulsive. It is interesting to see that the exotic $I = 3/2$ channel has a repulsive interaction. This seems to be a rather universal in this kind of studies [8, 19, 20].

I	S	Contact	ρ-exchange	D^*-exchange	$\sim$ Total$[I(J^P)]$
1/2	0	$+5g^2$	$-2\frac{g^2}{M_\rho^2}(k_1+k_3)\cdot(k_2+k_4)$	$-\frac{1}{2}\frac{\kappa g^2}{M_\rho^2}(k_1+k_4)\cdot(k_2+k_3)$	$-16g^2[1/2(0^+)]$
1/2	1	$+\frac{9}{2}g^2$	$-2\frac{g^2}{M_\rho^2}(k_1+k_3)\cdot(k_2+k_4)$	$+\frac{1}{2}\frac{\kappa g^2}{M_\rho^2}(k_1+k_4)\cdot(k_2+k_3)$	$-14.5g^2[1/2(1^+)]$
1/2	2	$-\frac{5}{2}g^2$	$-2\frac{g^2}{M_\rho^2}(k_1+k_3)\cdot(k_2+k_4)$	$-\frac{1}{2}\frac{\kappa g^2}{M_\rho^2}(k_1+k_4)\cdot(k_2+k_3)$	$-23.5g^2[1/2(2^+)]$
3/2	0	$-4g^2$	$+\frac{g^2}{M_\rho^2}(k_1+k_3)\cdot(k_2+k_4)$	$+\frac{\kappa g^2}{M_\rho^2}(k_1+k_4)\cdot(k_2+k_3)$	$+8g^2[3/2(0^+)]$
3/2	1	0	$+\frac{g^2}{M_\rho^2}(k_1+k_3)\cdot(k_2+k_4)$	$-\frac{\kappa g^2}{M_\rho^2}(k_1+k_4)\cdot(k_2+k_3)$	$+8g^2[3/2(1^+)]$
3/2	2	$+2g^2$	$+\frac{g^2}{M_\rho^2}(k_1+k_3)\cdot(k_2+k_4)$	$+\frac{\kappa g^2}{M_\rho^2}(k_1+k_4)\cdot(k_2+k_3)$	$+14g^2[3/2(2^+)]$

Table 1: $V(\rho D^* \to \rho D^*)$ for the different spin-isospin channels including the exchange of one heavy vector meson. The approximate Total is obtained at the threshold of ρD^*.

2.5 T-matrix

The results obtained in Tables 1, 2 and 3 provide the kernel or potential V to be used in the Bethe-Salpeter equation in its on-shell factorized form,

$$T = \frac{V}{1 - VG}\ , \tag{29}$$

I	S	Contact	ρ-exchange	D^*-exchange	$\sim$ Total$[I(J^P)]$
1/2	0	$-\sqrt{3}g^2$	-	$+\frac{\sqrt{3}}{2}\frac{\kappa\, g^2}{M_\rho^2}\,(k_1+k_4)\cdot(k_2+k_3)$	$0[1/2(0^+)]$
1/2	1	$+\frac{3\sqrt{3}}{2}g^2$	-	$-\frac{\sqrt{3}}{2}\frac{\kappa\, g^2}{M_\rho^2}\,(k_1+k_4)\cdot(k_2+k_3)$	$\frac{\sqrt{3}}{2}g^2[1/2(1^+)]$
1/2	2	$+\frac{\sqrt{3}}{2}g^2$	-	$+\frac{\sqrt{3}}{2}\frac{\kappa\, g^2}{M_\rho^2}\,(k_1+k_4)\cdot(k_2+k_3)$	$\frac{3\sqrt{3}}{2}g^2[1/2(2^+)]$

Table 2: $V(\rho D^* \to \omega D^*)$ for the different spin-isospin channels including the exchange of one heavy vector meson. The approximate Total is obtained at the threshold of ρD^*.

I	S	Contact	ρ-exchange	D^*-exchange	$\sim$ Total$[I(J^P)]$
1/2	0	$-g^2$	-	$+\frac{1}{2}\frac{\kappa\, g^2}{M_\rho^2}\,(k_1+k_4)\cdot(k_2+k_3)$	$0[1/2(0^+)]$
1/2	1	$+\frac{3}{2}g^2$	-	$-\frac{1}{2}\frac{\kappa\, g^2}{M_\rho^2}\,(k_1+k_4)\cdot(k_2+k_3)$	$\frac{1}{2}g^2[1/2(1^+)]$
1/2	2	$+\frac{1}{2}g^2$	-	$+\frac{1}{2}\frac{\kappa\, g^2}{M_\rho^2}\,(k_1+k_4)\cdot(k_2+k_3)$	$\frac{3}{2}g^2[1/2(2^+)]$

Table 3: $V(\omega D^* \to \omega D^*)$ for the different spin-isospin channels including the exchange of one heavy vector meson. The approximate Total is obtained at the threshold of ρD^*.

for each spin-isospin channel independently. Here G is the two meson loop function

$$G = i\int \frac{d^4q}{(2\pi)^4}\frac{1}{q^2-m_1^2+i\epsilon}\frac{1}{(P-q)^2-m_2^2+i\epsilon}\ , \tag{30}$$

which upon using dimensional regularization can be recast as

$$\begin{aligned} G &= \frac{1}{16\pi^2}\Big(\alpha + Log\frac{m_1^2}{\mu^2}+\frac{m_2^2-m_1^2+s}{2s}Log\frac{m_2^2}{m_1^2} \\ &+ \frac{p}{\sqrt{s}}\Big(Log\frac{s-m_2^2+m_1^2+2p\sqrt{s}}{-s+m_2^2-m_1^2+2p\sqrt{s}}+Log\frac{s+m_2^2-m_1^2+2p\sqrt{s}}{-s-m_2^2+m_1^2+2p\sqrt{s}}\Big)\Big)\ , \end{aligned} \tag{31}$$

where P is the total four-momentum of the two mesons, p is the three-momentum of the mesons in the center-of-mass frame. Analogously, using a cut off one obtains

$$G = \int_0^{q_{max}} \frac{q^2dq}{(2\pi)^2}\frac{\omega_1+\omega_2}{\omega_1\omega_2[(P^0)^2-(\omega_1+\omega_2)^2+i\epsilon]}\ , \tag{32}$$

where q_{max} stands for the cut off, $\omega_i = (\vec{q}_i^{\,2}+m_i^2)^{1/2}$ and the center-of-mass energy $\left(P^0\right)^2 = s$.

Equation (29) in $I = 1/2$ is a 2×2 matrix equation with the amplitudes $\rho D \to \rho D$, $\rho D \to \omega D$ and $\omega D \to \omega D$ in the elements $(1,1)$, $(1,2)$ and $(2,2)$.

The formalism that we are using is also allowed for s-channel ρ or D exchange and we can have the diagram of Fig. 6. But we found in [4] that this leads to a p-wave interaction for equal masses of the vectors, and only to a minor component of s-wave in the case of different masses [8].

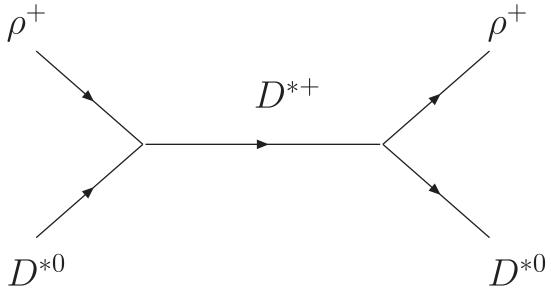

Figure 6: S-channel D^* exchange diagram.

3 Convolution due to the ρ mass distribution

The strong attraction in the $I = 1/2$ and $S = 0, 1, 2$ channels will produce ρD^* bound states with no width within the present treatment so far. However, this is not strictly true because the ρ meson has a large width or equivalently a mass distribution that allows the states obtained to decay in ρD^* for the low mass components of the ρ mass distribution. To take this into account we follow the traditional method which is to convolute the G function for the mass distribution of the ρ meson [14] replacing the G function by $\tilde{G}$ as follows

$$\tilde{G}(s) \;=\; \frac{1}{N}\int_{(m_\rho-2\Gamma_\rho)^2}^{(m_\rho+2\Gamma_\rho)^2} d\tilde{m}_1^2(-\frac{1}{\pi})\mathcal{I}m\frac{1}{\tilde{m}_1^2-m_\rho^2+i\Gamma\tilde{m}_1}G(s,\tilde{m}_1^2,m_{D^*}^2)\ , \tag{33}$$

with

$$N=\int_{(m_\rho-2\Gamma_\rho)^2}^{(m_\rho+2\Gamma_\rho)^2} d\tilde{m}_1^2(-\frac{1}{\pi})\mathcal{I}m\frac{1}{\tilde{m}_1^2-m_\rho^2+i\Gamma\tilde{m}_1}\ , \tag{34}$$

where $\Gamma_\rho = 146.2\,MeV$ and for $\Gamma \equiv \Gamma(\tilde{m})$ we take the ρ width for the decay into the pions in p-wave

$$\Gamma(\tilde{m}) = \Gamma_\rho(\frac{\tilde{m}^2-4m_\pi^2}{m_\rho^2-4m_\pi^2})^{3/2}\theta(\tilde{m}-2m_\pi)\ . \tag{35}$$

The use of $\tilde{G}$ in Eq. (29) provides a width to the states obtained as we will see in the next section.

4 Results

When one introduces the amplitudes obtained in Tables 1, 2 and 3 as a kernel V in Eq. (29), one finds bound states with zero width in the three different cases $I = 1/2$ and $S = 0, 1, 2$. The pole positions are given in Table 4. In Eq. (31) we have fixed the value of μ as $1500\,MeV$ and we have fine tuned the subtraction constant, α, around its natural value of -2 [21] in order to get the position of the $S = 2$ resonance at its value of the PDG. To

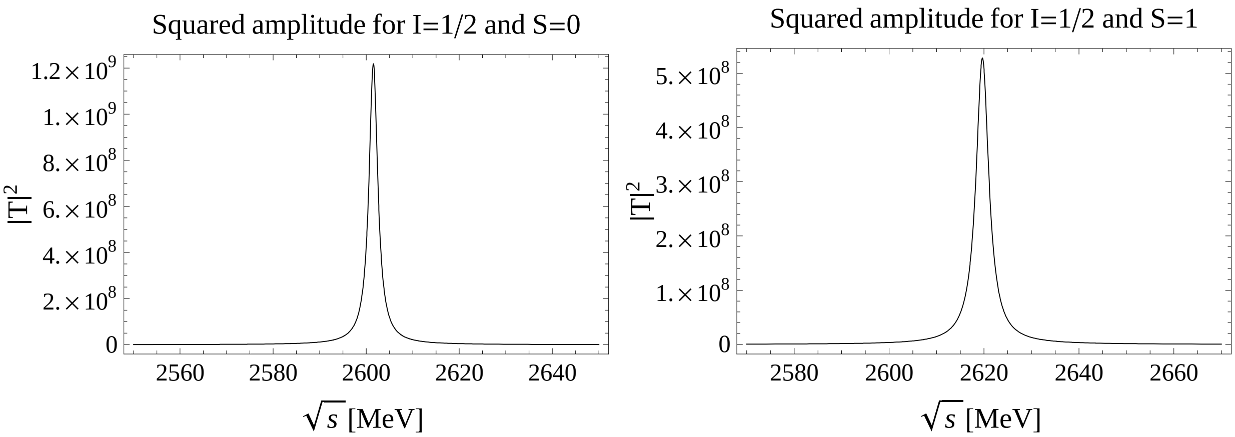

Figure 7: Squared amplitude for $I = 1/2$ and $S = 0, 1$ including the convolution of the ρ-mass distribution.

quantify the freedom one has in this fine tuning we quote that the value of the mass that we obtain using $\alpha = -2$, is $2346\,MeV$. The value of α for the pole positions given in the Table 4 is -1.74.

I	S	$\sqrt{s}\ (MeV)$
1/2	0	2592
1/2	1	2611
1/2	2	2450

Table 4: Pole positions for the three different cases

As it was explained in the previous section, the loop function G must be convoluted to take into account the width of the ρ meson. When we do it, we find bound states with a small width as we can see in Figs. 7 and 8. In fact, the widths found are $\sim 5\,MeV$, $4\,MeV$, and $0\,MeV$ for $S = 0, 1$ and 2, respectively.

In Eq. (29), the amplitude close to a pole looks like

$$T_{ij} \approx \frac{g_i g_j}{z - z_R}\ , \tag{36}$$

where $Re\, z_R$ gives the mass of the resonance and $Im\, z_R$ the half width. The constants g_i ($i = \rho D^*,\ \omega D^*$), which provide the coupling of the resonance to one particular channel, can be calculated by means of the residues of the amplitudes as given in Table 5. In the PDG [6], two states are listed, $D^*(2640)$ and $D_2^*(2460)$ in the sectors $I(J^P) = 1/2(?^?)$ and $I(J^P) = 1/2(2^+)$, respectively. Comparing with the present model predictions as listed in Table 4, we attempt to identify them with those states of $S = 1$ and $S = 2$, respectively. The reason to identify the $D^*(2640)$ with our pole for the case of $S = 1$ and not $S = 0$ is going to be clear in the next section when the $D\pi$ channel is considered. In the case of

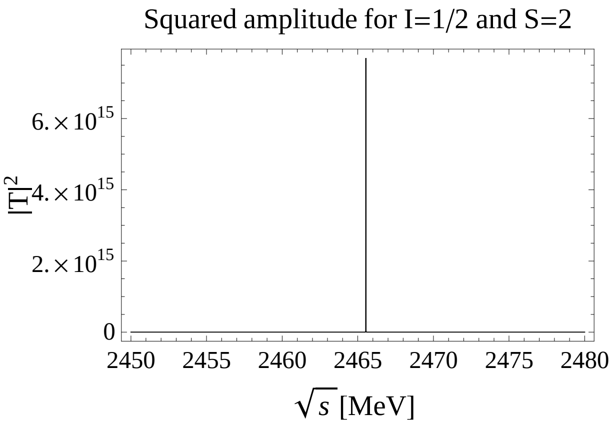

Figure 8: Squared amplitude for $I = 1/2$ and $S = 2$ including the convolution of the ρ-mass distribution.

the $D^*(2640)$ the width quoted in the PDG is very small, $\Gamma < 15\,MeV$. According to our result after taking into account the ρ mass distribution, one obtains 3–4 MeV, see Fig. 7. In the case of $D_2^*(2460)$, the width quoted in the PDG is $43 \pm 4\,MeV$ for the D_2^{*0} and $37 \pm 6\,MeV$ for $D_2^{*\pm}$. Then, it is clearly not compatible with the width found here, which is zero, see Fig. 8, and we need to allow that the resonance decays to another channel. For this reason we are going to consider the $D\pi$ channel in the next section, which is below the threshold of ρD^*. A novelty in this work is that we have obtained a new resonance in the sector $I = 1/2$ and $S = 0$ which does not appear in the PDG, see Table 4. One should note that if one takes Eq. (32) instead of the Eq. (31) with a cutoff of the order of the natural size $q_{max} = 1$–$1.2\,GeV$, the results are very similar to those of Table 4 (difference around 1%), which is an indication of the stability of the results.

Channel	$D_0^*(2600)$	$D_1^*(2640)$	$D_2^*(2460)$
ρD^*	14.32	14.04	17.89
ωD^*	0.53	1.40	2.35

Table 5: Modules of the couplings g_i in units of GeV for the poles in the $S = 0,\ 1,\ 2;\ I = 1/2$ sector with the channel ρD^* and ωD^*.

5 The πD decay mode

5.1 Evaluation of the πD-box diagram

In the previous section we have obtained the positions of the poles and obtained a small width for the states taking into account the finite width of ρ. Here we consider a dominant decay mode into the πD channel in order to give account of a finite width. Our starting point is the set of diagrams of Fig. 9. One needs the $\rho\pi\pi$ and the $D^*\pi D$ vertex which are provided within the same hidden gauge formalism [1], [2], used in Section 2, by means of the Lagrangian

$$\mathcal{L}_{V\Phi\Phi} = -ig\langle V^\mu[\Phi, \partial_\mu\Phi]\rangle \ . \tag{37}$$

For the first diagram of Fig. 9 we have:

$$\begin{aligned} -\,it^{(\pi D)} &= \int \frac{d^4q}{(2\pi)^4}(-i)^4\, g^4(\sqrt{2})^2\,(\frac{1}{\sqrt{2}})^2\,(k_1-2q)^\mu\epsilon^{(1)}_\mu \\ &\times\ (k_3-2q)^\nu\epsilon^{(3)}_\nu(P+k_1-2q)^\alpha\epsilon^{(2)}_\alpha(P+k_3-2q)^\beta\epsilon^{(4)}_\beta \\ &\times\ \frac{i}{q^2-m_\pi^2+i\epsilon}\,\frac{i}{(k_1-q)^2-m_\pi^2+i\epsilon} \\ &\times\ \frac{i}{(P-q)^2-m_D^2+i\epsilon}\,\frac{i}{(k_3-q)^2-m_\pi^2+i\epsilon}\ . \end{aligned} \tag{38}$$

Using the approximation that all the polarization vectors are spatial, it is possible to write the above amplitude as

$$\begin{aligned} -\,it^{(\pi D)} &= g^4\int\frac{d^4q}{(2\pi)^4}16\,q_iq_jq_lq_m\,\epsilon^{(1)}_i\epsilon^{(2)}_j\epsilon^{(3)}_l\epsilon^{(4)}_m \\ &\times\ \frac{1}{q^2-m_\pi^2+i\epsilon}\,\frac{1}{(k_1-q)^2-m_\pi^2+i\epsilon} \\ &\times\ \frac{1}{(P-q)^2-m_D^2+i\epsilon}\,\frac{1}{(k_3-q)^2-m_\pi^2+i\epsilon}\ . \end{aligned} \tag{39}$$

This integral is logarithmically divergent and as in [4] we regularize it with a cutoff in the three-momentum of the order of the natural size, for which we take $q_{max} = 1.2\,GeV$. The results do not change much if one takes a value around this. After performing the dq^0 integral of Eq. (39), one finds

$$\begin{aligned} V^{(\pi D)} &= g^4\,\left(\epsilon^{(1)}_i\epsilon^{(2)}_i\epsilon^{(3)}_j\epsilon^{(4)}_j+\epsilon^{(1)}_i\epsilon^{(2)}_j\epsilon^{(3)}_i\epsilon^{(4)}_j+\epsilon^{(1)}_i\epsilon^{(2)}_j\epsilon^{(3)}_j\epsilon^{(4)}_i\right) \\ &\times\ \frac{8}{15\pi^2}\int_0^{q_{max}}dq\,\vec{q}^{\,6}\,\left(\frac{1}{2\omega}\right)^3\left(\frac{1}{k_1^0+2\omega}\right)^2\frac{1}{k_2^0-\omega-\omega_D+i\epsilon} \\ &\times\ \frac{1}{k_4^0-\omega-\omega_D+i\epsilon}\,\frac{1}{k_1^0-2\omega+i\epsilon}\,\frac{1}{k_3^0-2\omega+i\epsilon}\,\frac{1}{P^0-\omega-\omega_D+i\epsilon} \\ &\times\ \frac{1}{P^0+\omega+\omega_D}\left(\frac{1}{k_2^0+\omega+\omega_D}\right)^2\frac{1}{2\omega_D}\,f(P^0) \end{aligned} \tag{40}$$

where

$$
\begin{aligned}
f(P^0) = \quad & 4 \quad \{-32 k_3^0 P^0 \omega^2 \omega_D ((P^0)^2 - 2\omega^2 - 3\omega\omega_D - \omega_D^2) \\
+ \quad & 2(k_3^0)^3 P^0 \omega_D ((P^0)^2 - 5\omega_D^2 - 2\omega\omega_D - \omega_D^2) \\
+ \quad & (k_3^0)^4 (2\omega^3 - (P^0)^2 \omega_D + 3\omega^2\omega_D + 2\omega\omega_D^2 + \omega_D^3) \\
+ \quad & 4\omega^2 (8\omega^5 + 33\omega^4\omega_D + 54\omega^3\omega_D^2 + 3\omega_D((P^0)^2 - \omega_D^2)^2 \\
+ \quad & 18\omega\omega_D^2(-(P^0)^2 + \omega_D^2) + \omega^2(-12\ (P^0)^2\omega_D + 44\omega_D^3)) \\
- \quad & (k_3^0)^2 (16\omega^5 + 63\omega^4\omega_D + 74\omega^3\omega_D^2 + \omega_D((P^0)^2 - \omega_D^2)^2 \\
+ \quad & 32\omega^2\omega_D(-(P^0)^2 + \omega_D^2) + \omega(-6(P^0)^2\ \omega_D^2 + 6\omega_D^4))\} \qquad (41)
\end{aligned}
$$

and $\omega = \sqrt{\vec{q}^{\,2} + m_\pi^2}$, $\omega_D = \sqrt{\vec{q}^{\,2} + m_D^2}$, $P^0 = k_1^0 + k_2^0$. In Eq. (40) we can see clearly the sources of the imaginary part in the cuts $k_2^0(k_4^0) - \omega - \omega_D = 0$, $k_1^0(k_3^0) - 2\omega = 0$, $P^0 - \omega - \omega_D = 0$, which give rise to the decays $D^{*0} \to \pi D$, $\rho \to \pi\pi$ and $\rho D^{*0} \to \pi D$ respectively. As in [4], to take into account the ρ mass distribution, we make a simple approach. First we neglect the three-momenta of external particles ($\vec{k}_i \sim 0$, i =1, 2, 3, 4) and approximate $k_1^0 \sim k_3^0 \sim m_\rho$ and $k_2^0 \sim k_4^0 \sim m_{D^*}$. Then we find double poles of $(1/(k_1^0 - 2\omega + i\epsilon))^2$ and $(1/(k_2^0 - \omega - \omega_D + i\epsilon))^2$. These double poles are then removed by replacing

$$
\left(\frac{1}{k_1^0 - 2\omega + i\epsilon}\right)^2 \to \frac{1}{k_1^0 - 2\omega + i\Gamma_\rho/4}\ \frac{1}{k_1^0 - 2\omega - i\Gamma_\rho/4} \qquad (42)
$$

and so on, considering a finite width for ρ and D^*. Here we set $\Gamma_\rho = 146.2\,MeV$ and $\Gamma_{D^*} = 2.1\,MeV$ (results are identical if we put $\Gamma_{D^*} = 0\,MeV$). Once this is done, the other diagrams of Fig. 9 are calculated easily, which takes into account the decay into the πD channel. One must make a projection into a proper isospin and spin. For isospin, only $I = 1/2$ is allowed, while for spin, $S = 0$ and 2 are allowed. Decay into $S = 1$ is forbidden since the parity of the ρD^* system for ρ in s wave is positive, which forces the πD system to be in $L = 0, 2$. Since the π and D have no spin, the total angular momentum J is equal to L in this case. Therefore, only the 0^+, 2^+ quantum numbers have this decay channel. This provides an explanation on why the $D^*(2640)$ does not have practically width and the $D_2^*(2460)$ has a bigger width. Finally, we obtain

$$
\begin{aligned}
t^{(2\pi, I=1/2, S=0)} &= 20\,\tilde{V}^{(\pi D)}\ , \\
t^{(2\pi, I=1/2, S=2)} &= 8\,\tilde{V}^{(\pi D)}\ , \qquad (43)
\end{aligned}
$$

where $\tilde{V}^{(\pi D)}$ is given by Eq. (40) after removing the polarization vectors. As in [4] we use a form factor for a off-shell π in each vertex, which is

$$
F(q) = \frac{\Lambda^2 - m_\pi^2}{\Lambda^2 + \vec{q}^{\,2}}\ , \qquad (44)
$$

with $\Lambda = 1400, 1500\,MeV$. The real and imaginary parts of the potential for the contributions that we have calculated are plotted in Figs. 10 and 11. As we can see, the real part of the potential coming from the πD-box diagram is much smaller than the real part of the potential coming from the contact plus exchange terms.

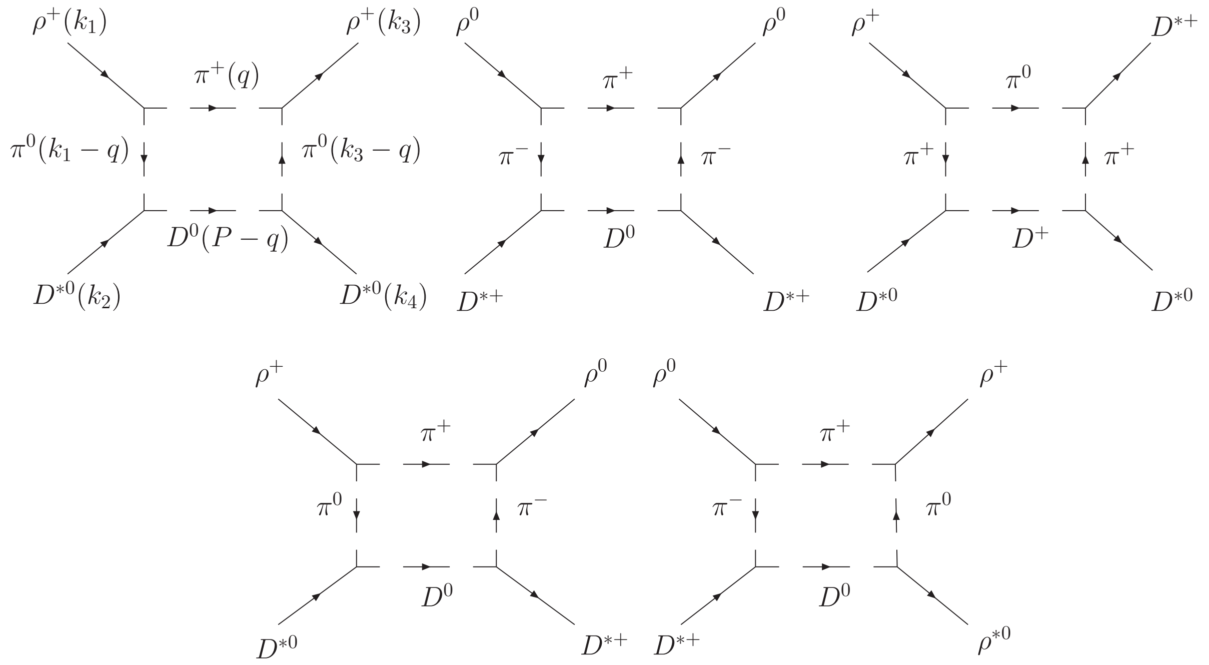

Figure 9: πD-box diagrams

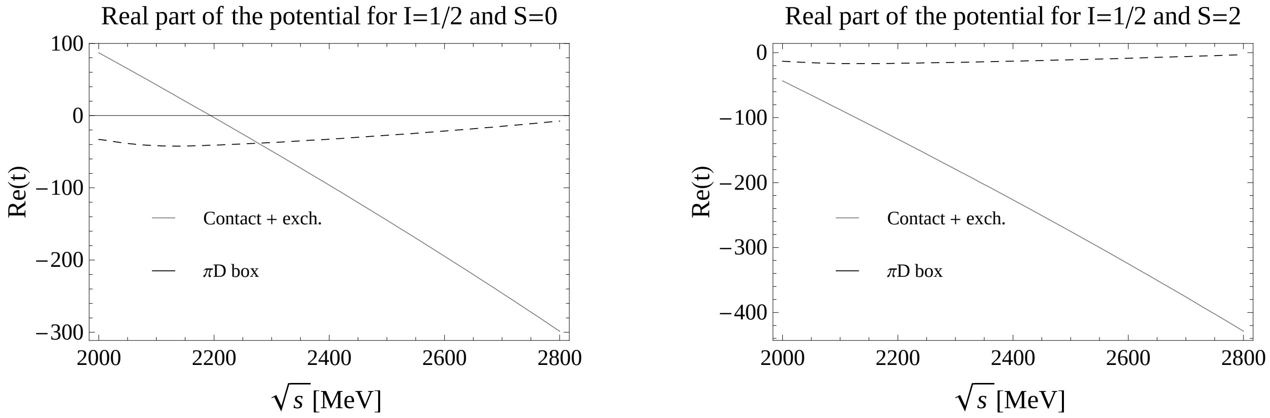

Figure 10: Real part of the potential for $I = 1/2$; $S = 0$; and $I = 1/2; S = 2$;.

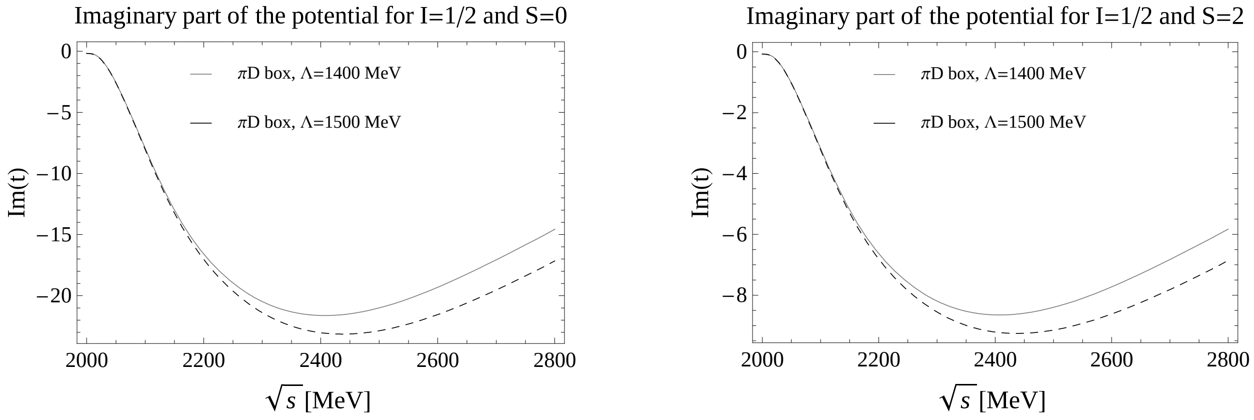

Figure 11: Imaginary part of the potential for $I = 1/2$; $S = 0$; and $I = 1/2; S = 2$;.

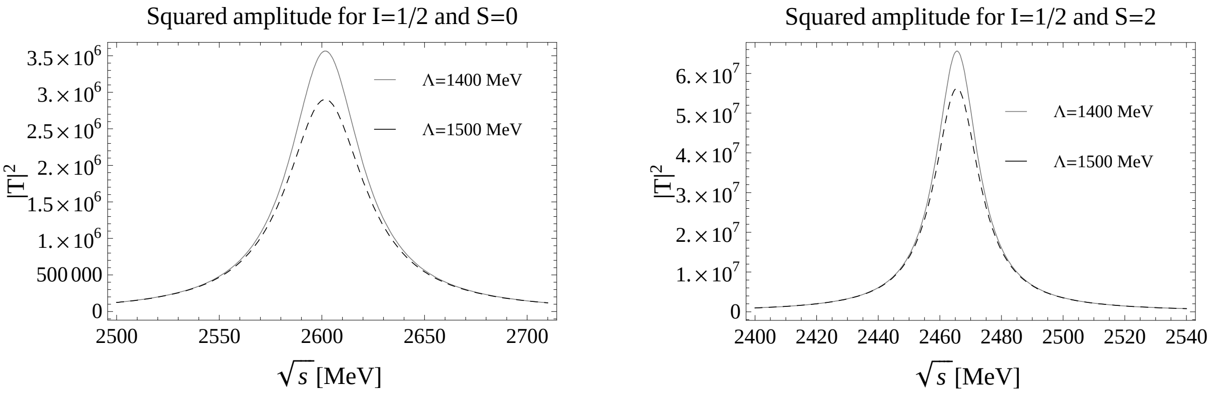

Figure 12: Squared amplitude for $S = 0$ and $S = 2$ including the convolution of the ρ-mass distribution and the πD-box diagram.

5.2 Results with $V^{(\pi D)}$

In Fig. 12 we show the results when one introduces the amplitudes of the Tables 1, 2, 3 and the given ones in Eqs. (43) and (40) in the Bethe-Salpeter equation Eq. (29). As one can see, now the states for $S = 0$ and $S = 2$ have larger width since they can decay to πD also. We have found a width of $20\,MeV$ for the $D_2^*(2460)$, which is about 50% of the total width quoted in the PDG [6]. One could also have the $D^*\pi$ decay channel, which would be possible by means of a anomalous coupling but, as it was seen in [4], this leads to a smaller contribution than the other one. Also in the PDG the most important contribution comes from the πD channel. For the case of the new state found the width obtained is $50\,MeV$ with $\Lambda = 1500\,MeV$. In the next section we introduce new elements of phenomenology that help obtain a somewhat larger width.

5.3 Results with $V^{(\pi D)}$ using a different form factor and the experimental coupling constant $g_{D^*D\pi}$

In this section we would like to evaluate again the πD-box diagram, but, taking into account the strong coupling $g_{D^*D\pi}$ and a different form factor also for an off-shell pion. After the recent measurements by the CLEO Collaboration [22], it is known that the D^* meson couples strongly to $D\pi$. The experimental value of this coupling turns out to be larger, almost by a factor two, than the value obtained from some of the theoretical predictions using different approaches of the QCD sum rule [23, 24]. Within the hidden gauge formalism, the vertex $D^{*+}D^0\pi^-$ obtained from Eq. (37) is

$$\langle D^{*+}(p)\pi^-(q)|D^0(p+q)\rangle = -2\,g'_{D^*D\pi}q_\mu\epsilon^\mu \ , \tag{45}$$

with $g'_{D^*D\pi} = m_{D^*}/2f_D = 6.3$, which is also smaller than the experimental value for this, $g^{exp}_{D^*D\pi} = 8.95 \pm 0.15 \pm 0.95$. In [25], the $D^*D\pi$ form factor is evaluated using the QCD sum rule for a D or a π off-shell. A parameterization for an off-shell pion in terms of a form factor

$$F'(q^2) = g_{D^*D\pi}e^{q^2/\Lambda^2} \quad \text{with } \Lambda = 1.2\,GeV \ , \tag{46}$$

is taken, together with another form factor to account for off-shell D mesons, which we do not need here since we are concerned about the imaginary part of the box diagram where the D meson will be on-shell. In Eq. (46) q^2 is a four momentum square $q^2 = q^{0^2} - \vec{q}^2$. With these assumptions on the form factors, a value of $g_{D^*D\pi} = 2\,g'_{D^*D\pi} = 14.9$ is obtained in [25], which would be in better agreement with experiment ($g'_{D^*D\pi} = 7.45$).

For the first diagram of Fig. 9, we consider the q^0 component of the π^+ on-shell, hence $q_0 = \frac{s+m_\pi^2-m_D^2}{2\sqrt{s}} \sim 769.4\,MeV$ and $(k_1^0 - q^0) \sim 6\,MeV$, for ρD^* at threshold, in the approximation of momentum zero for external particles. This leads to $(k^0-q^0)^2/\Lambda^2 \sim 10^{-5}$, for values of Λ around $1\,GeV$. Then it is licit to use the three-momentum version of the form factor of the Eq. (46) for an off-shell pion in each of the vertices, that is, we replace in Eq. (40) the factor g^4 by

$$g^2_{\rho\pi\pi}\,(g^{exp}_{D^*D\pi})^2\,(e^{-\vec{q}^2/\Lambda^2})^4 \ , \tag{47}$$

with $g_{\rho\pi\pi} = m_\rho/2\,f_\pi = 4.2$ and $g^{exp}_{D^*D\pi} = 8.95\,MeV$ (the experimental value), $\Lambda \sim 1$–$1.2\,GeV$ and $\vec{q}$ running in the integral.

In Figs. 13 and 14 we show the real and imaginary parts of the potential using Eqs. (40) and (47). As we can see, the real part of the πD-box diagram is very small compared with those coming from the contact term plus vector exchange terms, and therefore we can ignore it, thus focusing our attention at the imaginary part. The imaginary part is now larger than that in Fig. 11, but is still comparable with the values quoted in the PDG [6] for the width. We show the $|T|^2$ in Fig. 15 for various cutoff parameters. The $|T|^2$ is similar to Fig. 12, but now the width is slightly larger. In the case of $\Lambda = 1\,GeV$, we obtain $40\,MeV$ for $S = 2$, very close to the value quoted by the PDG ($43 \pm 4\,MeV$), and $61\,MeV$ for $S = 0$. For $\Lambda = 1.2\,GeV$ we obtain for $S = 2$ a width around $60\,MeV$. Therefore, the two form factors, Eq. (44) and Eq. (47), provide reasonable values of the width, with a preference for the option using the experimental $g^{exp}_{D^*D\pi}$ value and $\Lambda = 1\,GeV$ in Eq. (47).

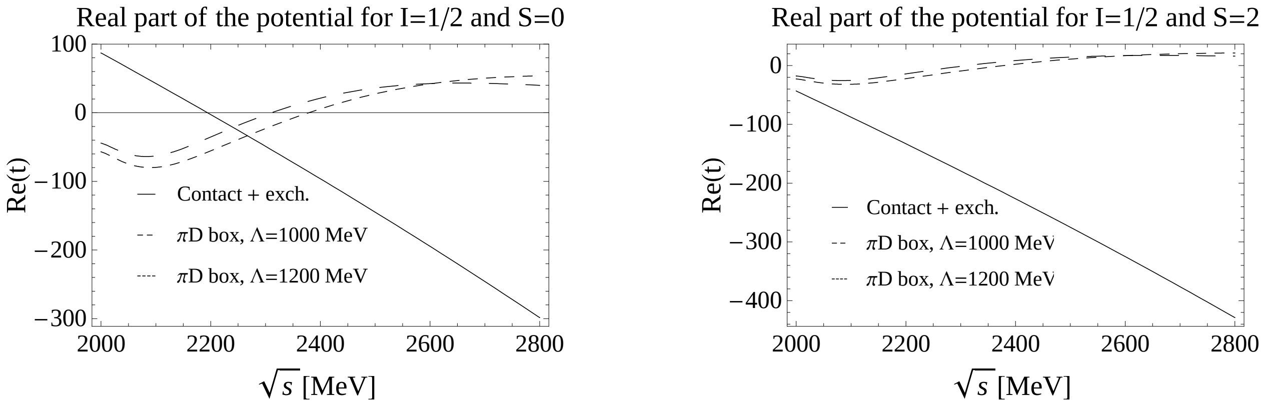

Figure 13: Real part of the potential for $I = 1/2$; $S = 0$; and $I = 1/2; S = 2$.

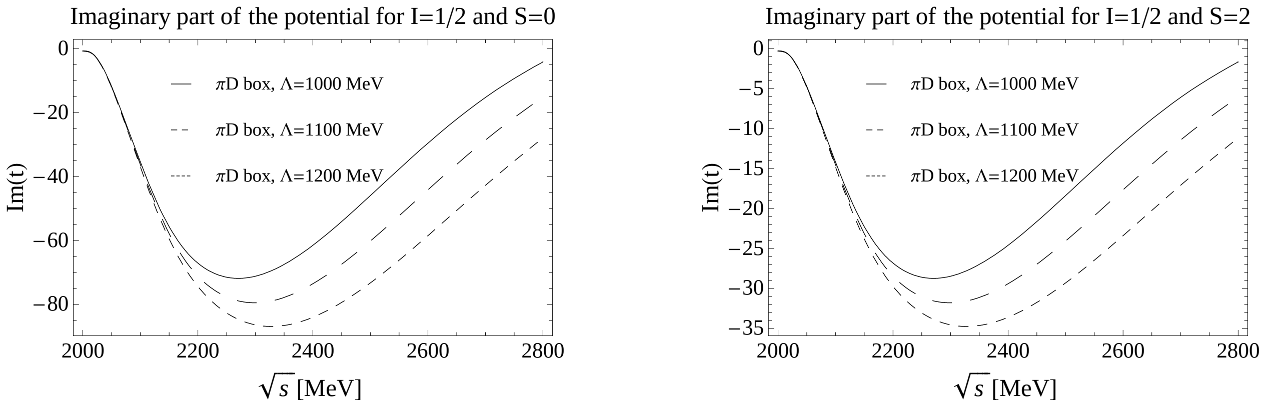

Figure 14: Imagiary part of the potential for $I = 1/2$; $S = 0$; and $I = 1/2; S = 2$.

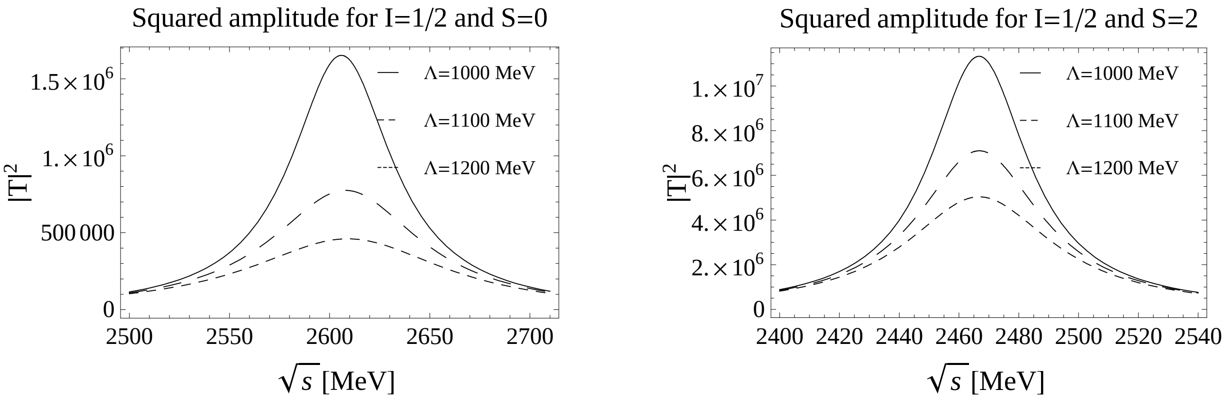
Squared amplitude for I=1/2 and S=0

Squared amplitude for I=1/2 and S=2

Figure 15: Squared amplitude for $S = 0$ and $S = 2$ including the convolution of the ρ-mass distribution and the πD-boxed diagram.

6 Conclusions

We have made a study of the $(\rho\omega)D^*$ interaction using the hidden gauge formalism. The interaction comes from contact terms plus ρ meson exchange in the t-channel. Of all spin and isospin allowed channels in s-wave, we found strong attraction, enough to bind the system, in $I = 1/2, S = 0$, $I = 1/2, S = 1$ and $I = 1/2, S = 2$. We also found that in the case of $I = 1/2, S = 2$ the interaction was more attractive, than in the other two cases, leading to a tensor state more bound than the scalar and the axial vector. The consideration of the ρ mass distribution gives a width to the three states, rather small in all cases. Consideration of the πD decay channel, in an equivalent way to what was done in the case of the $\rho\rho$ interaction going to $\pi\pi$ in [4], makes the widths larger and realistic. Yet, the smaller phase space available here makes this contribution relatively smaller than in the case of the $\rho\rho$ interaction. We found that the tensor state obtained matches the properties of the tensor state $D_2^*(2460)$. We predict two more states with $S = 0$ and $S = 1$, which are less bound than the tensor state. We find in the PDG the state $D^*(2640)$ without experimental spin and parity assigned, but we conjecture that this state should be the $S = 1$ state found by us because we could find a natural explanation for the small experimental width of this state. The other state nearly degenerate in energy with this one, but with spin $S = 0$, would still be to be found. The results obtained here should stimulate the search for more D states in the region of $2600\,MeV$.

Acknowledgments

This work is partly supported by DGICYT contract number FIS2006-03438. We acknowledge the support of the European Community-Research Infrastructure Integrating Activity Study of Strongly Interacting Matter (acronym HadronPhysics2, Grant Agreement n. 227431) under the Seventh Framework Programme of EU. A. H. is supported in part by the Grant for Scientific Research Contract No. 19540297 from the Ministry of Education, Culture, Science and Technology, Japan. H. N. is supported by the Grant for Scientific Research No. 18-8661 from JSPS.

References

[1] M. Bando, T. Kugo, S. Uehara, K. Yamawaki and T. Yanagida, Phys. Rev. Lett. **54**, 1215 (1985).

[2] M. Bando, T. Kugo and K. Yamawaki, Phys. Rept. **164**, 217 (1988).

[3] M. Harada and K. Yamawaki, Phys. Rept. **381**, 1 (2003) [arXiv:hep-ph/0302103].

[4] R. Molina, D. Nicmorus and E. Oset, arXiv:0809.2233 [hep-ph].

[5] H. Nagahiro, J. Yamagata-Sekihara, E. Oset and S. Hirenzaki, arXiv:0809.3717 [hep-ph].

[6] C. Amsler *et al.* [Particle Data Group], Phys. Lett. B **667**, 1 (2008).

[7] S. Uehara, private communication.

[8] L. S. Geng and E. Oset, arXiv:0812.1199v1 [hep-ph]

[9] C. Garcia-Recio, V. K. Magas, T. Mizutani, J. Nieves, A. Ramos, L. L. Salcedo and L. Tolos, arXiv:0807.2969 [hep-ph].

[10] L.S. Geng and J. Nieves, in preparation.

[11] J. Nieves, private communication.

[12] S. Godfrey and N. Isgur, Phys. Rev. D **32** (1985) 189.

[13] F. E. Close and E. S. Swanson, Phys. Rev. D **72**, 094004 (2005) [arXiv:hep-ph/0505206].

[14] H. Nagahiro, L. Roca, A. Hosaka and E. Oset, Phys. Rev. D **79** (2009) 014015 [arXiv:0809.0943 [hep-ph]].

[15] Riazuddin and Fayyazuddin, Phys. Rev. **147**, 1071 (1966).

[16] J.J. Sakurai, Currents and mesons (University of Chicago Press, Chicago Il 1969)

[17] J. Gasser and H. Leutwyler, Nucl. Phys. B **250**, 465 (1985).

[18] U. G. Meissner, Rept. Prog. Phys. **56**, 903 (1993) .

[19] T. Hyodo, D. Jido and A. Hosaka, Phys. Rev. D **75** (2007) 034002 [arXiv:hep-ph/0611004].

[20] T. Hyodo, D. Jido and A. Hosaka, Phys. Rev. Lett. **97** (2006) 192002 [arXiv:hep-ph/0609014].

[21] J. A. Oller and U. G. Meissner, Phys. Lett. B **500**, 263 (2001)

[22] S. Ahmed *et al.* [CLEO Collaboration], Phys. Rev. Lett. **87**, 251801 (2001)

[23] V. M. Belyaev, V. M. Braun, A. Khodjamirian and R. Ruckl, Phys. Rev. D **51**, 6177 (1995)

[24] P. Colangelo, G. Nardulli, A. Deandrea, N. Di Bartolomeo, R. Gatto and F. Feruglio, Phys. Lett. B **339**, 151 (1994)

[25] F. S. Navarra, M. Nielsen and M. E. Bracco, Phys. Rev. D **65** 037502 (2002)